



Published in final edited form as:

*Anal Chem.* 2010 January 1; 82(1): 197. doi:10.1021/ac901716d.

## Diffraction Detection of Proteins using Microbead-based Rolling Circle Amplification

Joonhyung Lee<sup>1,3</sup>, Kutay Icoz<sup>1,4</sup>, Ana Roberts<sup>6</sup>, Andrew D. Ellington<sup>6</sup>, and Cagri A. Savran<sup>1,2,4,5,\*</sup>

<sup>1</sup>Birck Nanotechnology Center, Purdue University, 1205 W State Street, West Lafayette, Indiana 47907

<sup>2</sup>School of Mechanical Engineering, Purdue University, 1205 W State Street, West Lafayette, Indiana 47907

<sup>3</sup>School of Chemical Engineering, Purdue University, 1205 W State Street, West Lafayette, Indiana 47907

<sup>4</sup>Weldon School of Biomedical Engineering, Purdue University, 1205 W State Street, West Lafayette, Indiana 47907

<sup>5</sup>School of Electrical and Computer Engineering, Purdue University, West Lafayette, Indiana 47907, USA

<sup>6</sup>Department of Chemistry and Biochemistry, University of Texas at Austin, 2500 Speedway, Austin, Texas 78712

### Abstract

We present a robust, sensitive, fluorescent or radio label-free self-assembled optical diffraction biosensor that utilizes rolling circle amplification (RCA) and magnetic microbeads as a signal enhancement method. An aptamer-based sandwich assay was performed on microcontact-printed streptavidin arranged in 15- $\mu\text{m}$ -wide alternating lines, and could specifically capture and detect platelet-derived growth factor B-chain (PDGF-BB). An aptamer served as a template for the ligation of a padlock probe and the circularized probe could in turn be used as a template for RCA. The concatameric RCA product hybridized to biotinylated oligonucleotides which then captured streptavidin-labeled magnetic beads. In consequence, the signal from the captured PDGF-BB was amplified via the concatameric RCA product, and the diffraction gratings on the printed areas produced varying intensities of diffraction modes. The detected diffraction intensity and the density of the microbeads on the surface varied as a function of PDGF-BB concentration. Our results demonstrate a robust biosensing platform that is easy to construct and use, and devoid of fluorescence microscopy. The self-assembled bead patterns allow both a visual analysis of the molecular binding events under an ordinary bright-field microscope and serve as a diffraction grating biosensor.

---

Detection of proteins in a sensitive and rapid manner plays an essential role in clinical applications. Numerous studies have been reported on using antibody-based immunoassay systems as recognition elements for detecting proteins.<sup>1-3</sup> Antibodies, however, are generally produced *in vivo*, which generates difficulties in engineering their properties. In contrast, aptamers, generated by an *in vitro* selection process, are single-stranded oligonucleotides (DNA or RNA) that can specifically bind and recognize a variety of analytes ranging from small organic molecules to proteins, even to whole cells. As a result, aptamers have been used

as recognition elements in a number of biosensing platforms.<sup>4-7</sup> However, even though aptamers uniquely transduce the recognition of analytes into the generation of readily observable signals, analytes in small quantities are still difficult to detect with aptamers alone, pointing to a need for novel signal enhancement schemes.

Among many other biosensing platforms, the effectiveness of optical diffraction based biosensors has been demonstrated for recognizing binding events of various biomolecules, which operate based on changes in effective height or refractive index on periodically patterned gratings.<sup>8-12</sup> In many studies, in order to detect small amount of biomolecules, additional signal enhancement was necessary.<sup>13</sup> The enhancement was accomplished either by microfabrication of solid diffraction gratings or by *in situ* assembled diffraction gratings that are self-fabricated by nano or micro-size particles. Compared to the microfabrication of diffraction gratings which increases cost, time and in some cases requirement of additional amplification steps, the microbead-based *in situ* assembled diffraction grating enables rapid, cost effective, and sensitive detection of biomolecular targets. The microbeads, due to their large size compared to target molecules, form self-assembled diffraction gratings, which significantly lowers analyte detection limits.<sup>13-15</sup> Nevertheless, the detection limit can be further improved by combination with novel and robust signal enhancement methods.

Rolling circle amplification (RCA) has been proven to enhance signals for detecting a variety of analytes due to its sensitivity.<sup>16-19</sup> Although polymerase chain reaction (PCR) also provides high sensitivity for the detection of various target molecules, RCA has some advantages over PCR. RCA, an isothermal technique, does not require expensive and/or relatively large-scale equipment for thermal cycling or special laboratory conditions to avoid contamination, which makes it adaptable to low-cost and robust biosensing. RCA requires a circular template and a primer with a free 3' end which is then extended via DNA or RNA polymerase with strand displacement abilities to result in a single stranded concatameric product consisting of tandem repeats of the complement of the circular template. The long concatameric product, thousands nucleotides in length, can be detected by a variety of methods such as hybridization of fluorescent-17, 18 or bead-labeled oligonucleotide probes.<sup>20-22</sup> In addition, RCA has been shown as a useful method for chip-based detection because the concatamers can be localized to a given spot on a microarray slide.<sup>23-26</sup> Herein we present a microbead-based RCA system as a signal enhancement method to achieve a sensitive self-assembled optical diffraction biosensor.

In this study, an aptamer-based sandwich assay in combination with RCA was used to detect platelet-derived growth factor B-chain (PDGF-BB) that is known to be related to tumor growth and transformation.<sup>27-30</sup> PDGF-BB was captured and sandwiched between two anti-PDGF-BB aptamers (Figure 1). The dimeric nature of the PDGF-BB molecule allowed using two aptamers with identical binding sequences with the secondary aptamer only having a DNA extension to serve as the primer. This extension was formed with considerable ease due to the aptamer itself being already a DNA. The biotinylated capture aptamer was immobilized on the surface where periodic patterns of streptavidin were microcontact printed using a polydimethylsiloxane (PDMS) stamp. The aptamer-primer complex acted as a primer for RCA to localize the RCA product directly to the PDGF. For our purposes, we have utilized a linear padlock probe in which the 15 nucleotides on the 3' end and 11 nucleotides on the 5' end hybridized to the 3' end sequence of the aptamer-primer complex and are ligated together to act as the circular template for RCA. The diffraction grating was then formed by introducing streptavidin-labeled beads that conjugated to biotinylated probes, which bound to RCA-amplified concatamers on the periodic patterns. Illuminating the pattern with a laser light produced diffraction modes with varying intensities that depended on the number of beads present on the patterns. Furthermore, in order to verify effectiveness of RCA on the periodical patterns as a signal enhancement method, we investigated the capability of an aptamer-based

sandwich assay without RCA on periodically patterned gratings. Given the small number of beads bound to the surface and hence the lack of observation of diffraction modes, RCA played an essential role in the sensitive detection of PDGF-BB.

## Experimental Section

### Materials

The following oligonucleotides were purchased from IDT (Coralville, IA). Capture aptamer labeled with biotin at 3' end was 5'-**TACTCAGGGCACTGCAAGCAAT TGTGGTCCCAATGGGCTGAGTATTTTTT**-biotin-3' (The boldface portion is the aptamer sequence). Aptamer-primer complex was 5'-**TACTCAGGGCACTGCAAGCAATTGTGGT CCAATGGGCTGAGTATTTTTTTGTCCGTGCTAGAAGGAAACAGTTAC**-3' (The boldface portion is the aptamer sequence and the italicized portion is the primer sequence.) and padlock probe was 5'-phosphate-*TAGCACGGACATATATGATGGACCGCAGTATGAGTA TCTCTATCACTACTAAGTGGAAAGAAATGTAAGTTCCTTC*-3' (The italicized portion is complementary to the italicized sequence of the aptamer-primer complex. Biotinylated oligonucleotide probe labeled with biotin at 5' end was 5'-biotin-GTTTCCTTCTAGCAC-3'. Streptavidin and PBS buffer were obtained from Invitrogen (Carlsbad, CA). PDGF-BB, -AA and -AB were purchased from R&D Systems (Minneapolis, MN). The PDGF proteins were reconstituted in 4mM HCl with 0.2% BSA (Invitrogen, Carlsbad, CA). Phi 29 reagent set and *E.coli* DNA ligase were purchased from Epicentre (Madison, WI). 750 nm diameter streptavidin-labeled magnetic beads were obtained from Thermo Fisher Scientific Inc. (Waltham, MA). Bovine serum albumin (BSA) was obtained from Sigma-Aldrich (St. Louis, MO)

### Construction of PDMS Stamps

Polydimethylsiloxane (PDMS) stamp with 15- $\mu\text{m}$ -wide alternating lines was prepared with a master mold having 15  $\mu\text{m}$  alternating stripes. Silicone elastomer base and curing agent (SYLGARD 184 silicone elastomer kit, Dow Corning Corp., Midland, MI) were mixed in a 10:1 ratio and degassed for 1 h. After pouring into the master mold, they were degassed for an additional hour. Curing was carried out at 65 °C overnight. The cured PDMS stamp was carefully peeled off the mold after cooling down to room temperature. The stamp was thoroughly rinsed with nanopure water and cleaned in a sonicator prior to use.

### Sandwich assay with RCA

On a gold-coated glass slide (50 nm thick gold with 5 nm thick chromium, Asylum Research), periodic patterns of streptavidin (1 mg/ml in PBS, 7.4 pH) were microcontact printed (contact time: 5 min) using a polydimethylsiloxane (PDMS) stamp with 15- $\mu\text{m}$ -wide alternating lines. After the streptavidin was microcontact-printed on the gold chip, the receptor-free stripes were blocked with 1 mg/ml of bovine serum albumin (BSA). After washing with 5 ml of PBS for 1 min (0.1 mM  $\text{Na}_2\text{HPO}_4$ , 1.8 mM  $\text{KH}_2\text{PO}_4$ , 137 mM NaCl, pH 7.4), 100  $\mu\text{L}$  of 1  $\mu\text{M}$  capture aptamer labeled with biotin at its 3' end in PBSM buffer (PBS, 2.7 mM KCl, 1 mM  $\text{MgCl}_2$ , pH 7.4) was allowed to conjugate to the printed area for 15 min. The aptamer was heat denatured at 95 °C for 3 min and cooled down to room temperature prior to the immobilization. After a 5 ml of PBSM wash for 1 min, 100  $\mu\text{L}$  of PDGF-BB (10 pM-100 nM in PBSM) was introduced and allowed to interact with the bound aptamer for 15 min at 37 °C. The surface was then rinsed with PBSM for 1 min, followed by the addition of 100  $\mu\text{L}$  of 2  $\mu\text{M}$  aptamer-primer complex in PBSM for 15 min at 37 °C. The aptamer-primer complex was also heat denatured at 95 °C for 3 min and cooled to room temperature prior to introduction to the chip. After a 5 ml of PBS wash for 1 min, 100  $\mu\text{L}$  of 2  $\mu\text{M}$  padlock probe in PBS was allowed to hybridize. The padlock

probe was designed so that the first 11 of nucleotides on the 5' end and the 15 of nucleotides on the 3' end were complementary to the primer moiety found on the aptamer-primer complex. Then, the padlock probe was circularized via ligation by 100  $\mu\text{L}$  of 10 units *E. coli* DNA ligase in ligation buffer (30 mM Tris-HCl (pH 8.0), 4 mM  $\text{MgCl}_2$ , 10 mM  $(\text{NH}_4)_2\text{SO}_4$ , 1.2 mM EDTA and 0.1 mM b-NAD) for 15 min at 37°C forming the circular template for RCA. The complex was incubated with 50  $\mu\text{L}$  of 50 U phi29 DNA polymerase and 1.0 mM dNTPs in RCA reaction buffer (40 mM Tris-HCl (pH 7.5), 50 mM KCl, 10 mM  $\text{MgCl}_2$ , 5 mM  $(\text{NH}_4)_2\text{SO}_4$  and 4 mM DTT). The RCA reaction was conducted for 10 min at 37 °C, followed by a 5 ml of PBS rinse step for 2 min. 100  $\mu\text{L}$  of 2.5  $\mu\text{M}$  probe (biotinylated at 5'end) was heat denatured at 95 °C for 3 min and cooled down to room temperature. It was then applied to the surface and allowed to hybridize with the immobilized concatameric RCA products. 10  $\mu\text{L}$  of streptavidin-labeled beads (1 % solid concentration/mL, 0.75  $\mu\text{m}$  diameter) were suspended in PBS, placed in a magnetic separator, washed with 200  $\mu\text{l}$  of PBS for 2 min three times and resuspended in 100  $\mu\text{l}$  of PBS prior to use. The streptavidin-labeled beads were then allowed to conjugate to the biotinylated probes already hybridized to the RCA product. Finally, the chip was washed with 5 ml of PBS for 1 min, followed by a quick (~10 sec) wash with 5 ml of ammonium acetate buffer (300 mM  $\text{CH}_3\text{COONH}_4$ , pH 7.0).

### Sandwich assay without RCA

After the streptavidin was microcontact-printed on the gold chip, the receptor-free stripes were blocked with 1 mg/ml of bovine serum albumin (BSA). After washing with 5 ml of PBS for 1 min, 100  $\mu\text{L}$  of 1  $\mu\text{M}$  capture aptamer labeled with biotin at its 3'end was conformationally equilibrated by heating to 95 °C for 3 min followed by cooling to room temperature. The aptamer was incubated on the chip for 15 min in PBSM. After a 5 ml of PBSM wash for 1 min, 100  $\mu\text{L}$  of PDGF-BB (1 nM in PBSM) was introduced and allowed to interact with the bound aptamer for 15 min. The surface was then rinsed with PBSM for 1 min, followed by the addition of 100  $\mu\text{L}$  of 2  $\mu\text{M}$  conformationally equilibrated capture aptamer labeled with biotin at its 3' end in PBSM buffer for 30 min at 37 °C. The streptavidin-labeled beads then captured the biotinylated aptamers. Finally, the chip was washed with 5 ml of PBS for 1 min, followed by a quick wash with 5 ml of ammonium acetate buffer (300 mM  $\text{CH}_3\text{COONH}_4$ , pH 7.0).

### Diffraction Setup

A laser beam (He-Ne laser, Newport R-30991, 633 nm, 5 mW) passed through a beam splitter (Thorlabs, BS016) and a convex lens (focal length 60 mm), leading to an incident beam diameter of approximately 150  $\mu\text{m}$  on the gold surface. The reflected beam passed through a beam splitter, focused onto a CCD camera (Thorlabs, DCU223C). The measured signal intensities were recorded by a computer. Since the 0th mode was too intense, the exposure time of the CCD was set to 4.462 ms, and a band pass filter (Thorlabs, FB620-10) was placed between the laser and the beam splitter to decrease the intensity of this mode. On the other hand, a CCD exposure time of 0.398 ms was used for measuring the 1st mode intensity.<sup>13, 15</sup>

## Results and Discussion

### Detection of PDGF-BB via RCA

Figure 1 (a) illustrates the sandwich assay procedure, including the capture aptamer, PDGF-BB, the aptamer complex, and the subsequent microbead-based signal enhancement strategy. Periodic patterns of streptavidin were microcontact printed using a PDMS stamp with 15- $\mu\text{m}$ -wide alternating lines. Biotinylated capture aptamers were then adhered to the streptavidin coated lines. PDGF was washed over the surface and bound to the capture aptamer. A secondary aptamer bound to the immobilized protein in a classic sandwich assay format. Both the 3' and 5' ends of a padlock probe could hybridize to the 3' end of the secondary aptamer. Ligation of the padlock probe resulted in a circular template for RCA, with the 3' end of the secondary

aptamer acting as a primer. The requirement for ligation adds an additional layer of specificity, suppresses background, and therefore increases sensitivity, similar to how the proximity ligation assay increases sensitivity.<sup>31, 32</sup> The concatamers that accumulated as a result of RCA were thus effectively immobilized on 15- $\mu\text{m}$ -wide alternating lines. Multiple probes could hybridize to the long concatameric product. By conjugating biotinylated probes to streptavidin-coated microbeads it proved possible to obtain visual confirmation of the binding reaction, as well as diffractometric detection. In addition, the fact that a single bead might be bound by multiple repeats of the concatamer meant that we did not have to pre-optimize the binding affinity of the oligonucleotide probe to a given bead. As shown in Figure 1(b), self-assembled microbeads on the RCA-amplified concatamers formed gratings that produced diffraction modes upon illumination with a laser. The self-assembled diffraction gratings were examined under an optical microscope as shown in Figure 2 and were subjected to diffraction measurements.

### Dependence of normalized diffraction mode intensities on PDGF-BB concentration

Illuminating the grating formed by the streptavidin-coated microbeads yielded diffraction modes due to interference of the laser beams that reflected from the beads and the bead-free gold surface. We investigated the dependence of normalized diffraction mode intensities ( $I_1/I_0$ , a ratio of first mode  $I_1$  to zeroth mode  $I_0$ ) as a function of applied PDGF-BB concentration. The normalization was performed to suppress the disturbances that are known to influence both modes similarly.<sup>13-15</sup> To investigate a worst-case scenario, the measurement was carried out on 5 different areas of each chip to account for variations in bead packing between different areas. The averages and standard deviations were calculated offline. Figure 3 demonstrates the dependence of the normalized diffraction intensity on the concentration of PDGF-BB. As the concentration of PDGF-BB increased from 10 pM to 100 nM so did the number of beads that bound to the printed areas, resulting in a corresponding increase in the normalized modal intensity. Fitting a Langmuir isotherm relation to our dose/response curve yields a dissociation constant of 0.8 nM. This value is comparable to that reported elsewhere (0.1 nM<sup>33, 34</sup>), but may be slightly higher due to surface effects. The minimum detectable concentration was 10 pM, beyond which the diffraction intensity was too weak to detect.

This minimum concentration is already better than what we reported in an earlier work that uses fluorescence-based detection scheme (0.4 nM).<sup>17</sup> A recent study that investigated protein detection using a combination of aptamers and quantum dot bioconjugates demonstrated a detection sensitivity of 0.4 nM.<sup>34</sup> Another study that used a commercial label-free electrochemical sensor in combination with thiolated PDGF aptamers and mercaptohexanol on a gold surface reported PDGF concentration in the range of 1-40 nM.<sup>28</sup> Our detection limit is lower by one to two orders of magnitude. On the other hand, the minimum detectable concentration of a commercial electrochemical immunosensor with aptamer-primed polymerase amplification was as low as 0.6 pM<sup>35</sup>, which is lower than our detection limit by more than an order of magnitude. Our system offers significant advantages in terms of cost, versatility and ease of construction: it can be built from scratch in most laboratory settings with virtually no fabrication (other than a PDMS stamp which can also be purchased) and applied to a wide range of targets. Further, it allows a direct 'visual check' of the resulting reaction by placing the chip under an ordinary bright-field microscope before performing a diffraction measurement.

### Dependence of bead packing density on PDGF-BB concentration

We also investigated the density of the streptavidin-labeled microbeads as a function of PDGF-BB concentration. This was done by counting the *differential* number: the number of beads on printed areas minus that on the adjacent non-printed stripes (i.e., non-specifically bound beads). For each investigated area, five printed stripes (15  $\mu\text{m}$   $\times$  150  $\mu\text{m}$ ) adjacent to five non-printed



stripes ( $15\ \mu\text{m} \times 150\ \mu\text{m}$ ) were considered. The counting was performed on five different areas ( $22500\ \mu\text{m}^2$ ) on the chip. Averages and standard variations were again calculated, and the standard deviations were similar to those in the previous diffraction measurements. The image processing for the bead counting was performed in MATLAB. Figure 4 demonstrates the dependence of the counted bead number on the PDGF-BB concentration in the range of  $10\ \text{pM}$  –  $100\ \text{nM}$ . The relationship was similar to that observed for the modal intensities shown in Figure 3. The diffraction measurement, however, was much simpler and quicker since it required measuring only two quantities ( $I_1$  and  $I_0$ ), whereas counting beads required image analysis of an entire area.

### Specificity of PDGF-BB detection with RCA

To validate the specificity of PDGF-BB detection, several control experiments were performed using dimeric isoforms of PDGF (PDGF-AA and AB,  $10\ \text{nM}$ ) as shown in Figure 5. In addition, a negative control was carried out in the absence of PDGF-BB. No significant numbers of beads were obtained in either the case of PDGF-AA or in the absence of PDGF-BB. PDGF-AB yielded slightly more beads than PDGF-AA, but the overall packing was very small in comparison with PDGF-BB. In an earlier study that did not involve sandwich assays, comparable results were obtained with PDGF-AB and -BB.<sup>29, 36</sup> Here, we observed much more specificity for PDGF-BB, which may be due to the additional discrimination afforded by the use of two aptamers in a sandwich assay.

Another negative control experiment (Figure 5) was carried out with  $10\ \text{nM}$  PDGF-BB, except that no RCA was performed. This data can be directly compared to the bead capture results described in Figure 2(b), but again resulted in a negligible number of beads on the printed area. These results effectively prove that the RCA-amplified concatamers were the templates for microbead capture, and thus that RCA was required to form the diffraction grating used for the detection of PDGF-BB.

### Variations in normalized diffraction intensities

To better understand the reasons for the variations in the normalized diffraction intensities, measurements were performed on a single spot for each chip (without moving to a different area on the chip). A reading was made three times on each spot, and averages and standard deviations were calculated. The variations in modal intensities were reduced significantly (compare Figure 3 and Figure 6). Hence, it is likely that a significant portion of the uncertainties in modal intensities are due to variations from one area to another within the same chip, and thus are due to imperfections in stamping or irregularities in the activities of immobilized molecules (i.e., due to surface denaturation). We are currently exploring alternative functionalization schemes involving lithography to improve the quality of the functional lines.

### Detection of PDGF-BB without RCA

In order to verify that RCA assisted with the sensitivity of optical diffraction methods, a control experiment was performed. Figure 7(a) shows a schematic of a microbead-based aptamer sandwich assay without RCA. After immobilization of the biotinylated aptamers on the periodic patterns of streptavidin, PDGF-BB was captured and biotinylated aptamers and streptavidin-coated magnetic beads were added. As shown in Figure 7 (b), the number of the beads on the periodic pattern with  $1\ \text{nM}$  PDGF-BB was significantly smaller than was seen with RCA (by a factor of 4 to 5). Furthermore, the diffraction gratings with  $1\ \text{nM}$  PDGF-BB didn't produce noticeable diffraction modes upon illumination with a laser light. Hence, it was confirmed that RCA can play an important role in signal amplification for optical diffraction sensing.

## Conclusions

In conclusion, we demonstrated that rolling circle amplification (RCA) in combination with microbeads can be used as a signal enhancement method to develop a sensitive self-assembled optical diffraction based biosensor. We sandwiched the dimer PDGF-BB with two aptamers and detected the presence of the analyte via RCA-based extension of the secondary aptamer and subsequent bead-based diffraction measurements. We showed that the density of the beads and the normalized diffraction intensity measured on the diffraction grating pattern depended monotonously on the PDGF-BB concentration. Aptamer-based sandwich assay without RCA did not result in significant bead-binding confirming the advantage of RCA. The detection of the RCA product was relatively simple and devoid of fluorescence or radio labels. Having established the proof-of-concept in this study, our future efforts will be focused on detection of disease makers present in various body fluids such as blood or serum, in conjunction with aptamer-based immunomagnetic separation.

## Acknowledgments

This work was supported by National Institute of Health (National Cancer Institute Innovative Molecular Analysis Technologies Program) under grant 5R21CA125473-02

## References

1. Wu GH, Datar RH, Hansen KM, Thundat T, Cote RJ, Majumdar A. *Nature Biotechnology* 2001;19:856–860.
2. Kim SJ, Gobi KV, Tanaka H, Shoyama Y, Miura N. *Chemistry Letters* 2006;35:1132–1133.
3. Henne WA, Doorneweerd DD, Lee J, Low PS, Savran C. *Analytical Chemistry* 2006;78:4880–4884. [PubMed: 16841906]
4. Savran CA, Knudsen SM, Ellington AD, Manalis SR. *Analytical Chemistry* 2004;76:3194–3198. [PubMed: 15167801]
5. Bini A, Centi S, Tombelli S, Minunni M, Mascini M. *Analytical and Bioanalytical Chemistry* 2008;390:1077–1086. [PubMed: 18066708]
6. Bini A, Minunni M, Tombelli S, Centi S, Mascini M. *Analytical Chemistry* 2007;79:3016–3019. [PubMed: 17338547]
7. Kirby R, Cho EJ, Gehrke B, Bayer T, Park YS, Neikirk DP, McDevitt JT, Ellington AD. *Analytical Chemistry* 2004;76:4066–4075. [PubMed: 15253644]
8. Jenison R, Yang S, Haeberli A, Polisky B. *Nature Biotechnology* 2001;19:62–65.
9. Goh JB, Loo RW, McAloney RA, Goh MC. *Analytical and Bioanalytical Chemistry* 2002;374:54–56. [PubMed: 12207241]
10. Goh JB, Tam PL, Loo RW, Goh MC. *Analytical Biochemistry* 2003;313:262–266. [PubMed: 12605863]
11. Peng LL, Varma MM, Regnier FE, Nolte DD. *Advanced Biomedical and Clinical Diagnostic Systems III* 2005;5692:224–232. 392.
12. Varma MM, Peng LL, Regnier FE, Nolte DD. *Imaging, Manipulation, and Analysis of Biomolecules and Cells: Fundamentals and Applications III* 2005;5699:503–510. 542.
13. Chang CL, Acharya G, Savran CA. *Applied Physics Letters* 2007;90
14. Acharya G, Chang CL, Holland DP, Thompson DH, Savran CA. *Angewandte Chemie-International Edition* 2008;47:1051–1053.
15. Acharya G, Chang CL, Doorneweerd DD, Vlashi E, Henne WA, Hartmann LC, Low PS, Savran CA. *Journal of the American Chemical Society* 2007;129:15824–15829. [PubMed: 18047330]
16. Schweitzer B, Roberts S, Grimwade B, Shao WP, Wang MJ, Fu Q, Shu QP, Laroche I, Zhou ZM, Tchernev VT, Christiansen J, Velleca M, Kingsmore SF. *Nature Biotechnology* 2002;20:359–365.
17. Yang LT, Fung CW, Cho EJ, Ellington AD. *Analytical Chemistry* 2007;79:3320–3329. [PubMed: 17378540]

18. Cho EJ, Yang LT, Levy M, Ellington AD. *Journal of the American Chemical Society* 2005;127:2022–2023. [PubMed: 15713061]
19. Soderberg O, Gullberg M, Jarvius M, Ridderstrale K, Leuchowius KJ, Jarvius J, Wester K, Hydbring P, Bahram F, Larsson LG, Landegren U. *Nature Methods* 2006;3:995–1000. [PubMed: 17072308]
20. Stromberg M, Goransson J, Gunnarsson K, Nilsson M, Svedlindh P, Stromme M. *Nano Letters* 2008;8:816–821. [PubMed: 18247520]
21. Schopf E, Fischer NO, Chen Y, Tok JBH. *Bioorganic & Medicinal Chemistry Letters* 2008;18:5871–5874. [PubMed: 18694640]
22. Beyer S, Nickels P, Simmel FC. *Nano Letters* 2005;5:719–722. [PubMed: 15826115]
23. Zhao WA, Ali MM, Brook MA, Li YF. *Angewandte Chemie-International Edition* 2008;47:6330–6337.
24. Hsu HY, Huang YY. *Biosensors & Bioelectronics* 2004;20:123–126. [PubMed: 15142584]
25. Nallur G, Luo CH, Fang LH, Cooley S, Dave V, Lambert J, Kukanskis K, Kingsmore S, Lasken R, Schweitzer B. *Nucleic Acids Research* 2001;29 art. no.-e118.
26. Hatch A, Sano T, Misasi J, Smith CL. *Genetic Analysis-Biomolecular Engineering* 1999;15:35–40. [PubMed: 10191983]
27. Lai RY, Plaxco KW, Heeger AJ. *Analytical Chemistry* 2007;79:229–233. [PubMed: 17194144]
28. Degefa TH, Kwak J. *Analytica Chimica Acta* 2008;613:163–168. [PubMed: 18395055]
29. Zhou L, Ou LJ, Chu X, Shen GL, Yu RQ. *Analytical Chemistry* 2007;79:7492–7500. [PubMed: 17722881]
30. Yang LT, Ellington AD. *Analytical Biochemistry* 2008;380:164–173. [PubMed: 18541130]
31. Pai SSEAD. *Methods Mol Biol* 2009;504:385–398. [PubMed: 19159107]
32. Pai SSEAD, Levy M. *Nucleic Acids Res* 2005;33:1–7. [PubMed: 15640442]
33. Huang CC, Huang YF, Cao Z, Tan W, Chang HT. *Anal Chem* 2005;77:5735–5741. [PubMed: 16131089]
34. Kim GI, Kim KW, Oh MK, Sung YM. *Nanotechnology* 2009;20:175503. [PubMed: 19420593]
35. Huang YNX, Gan S, Jiang J, Shen G, Yu R. *Analytical Biochemistry* 2008;382:16–22. [PubMed: 18675245]
36. Green LS, Jellinek D, Jenison R, Ostman A, Heldin CH, Janjic N. *Biochemistry* 1996;35:14413–14424. [PubMed: 8916928]



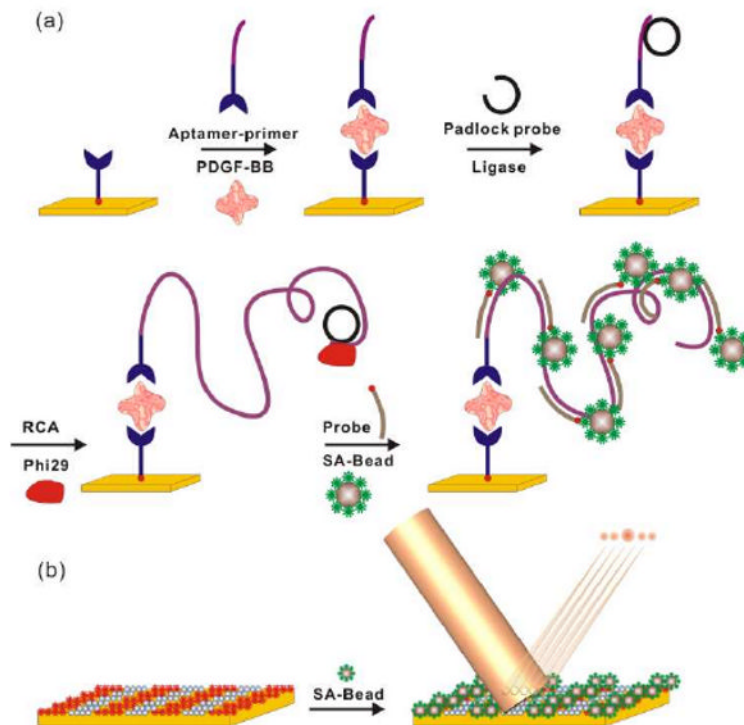


**Figure 1.**

(a) Schematic of RCA-based microbead detection assay in combination with aptamers. A biotinylated anti-PDGF-B specific aptamer is immobilized on streptavidin coated periodic patterns. PDGF-BB is introduced and captured by the aptamer. An aptamer-primer complex, with an additional primer sequence binds to the protein. A padlock probe hybridized to the primer tail of the aptamer is ligated and RCA is initiated. Streptavidin conjugated beads bind to elongated concatamers via hybridized biotinylated probes. (b) Self-assembled streptavidin (SA)-coated beads on the RCA-based micropattern form diffraction gratings that yield diffraction modes upon illumination with a laser.

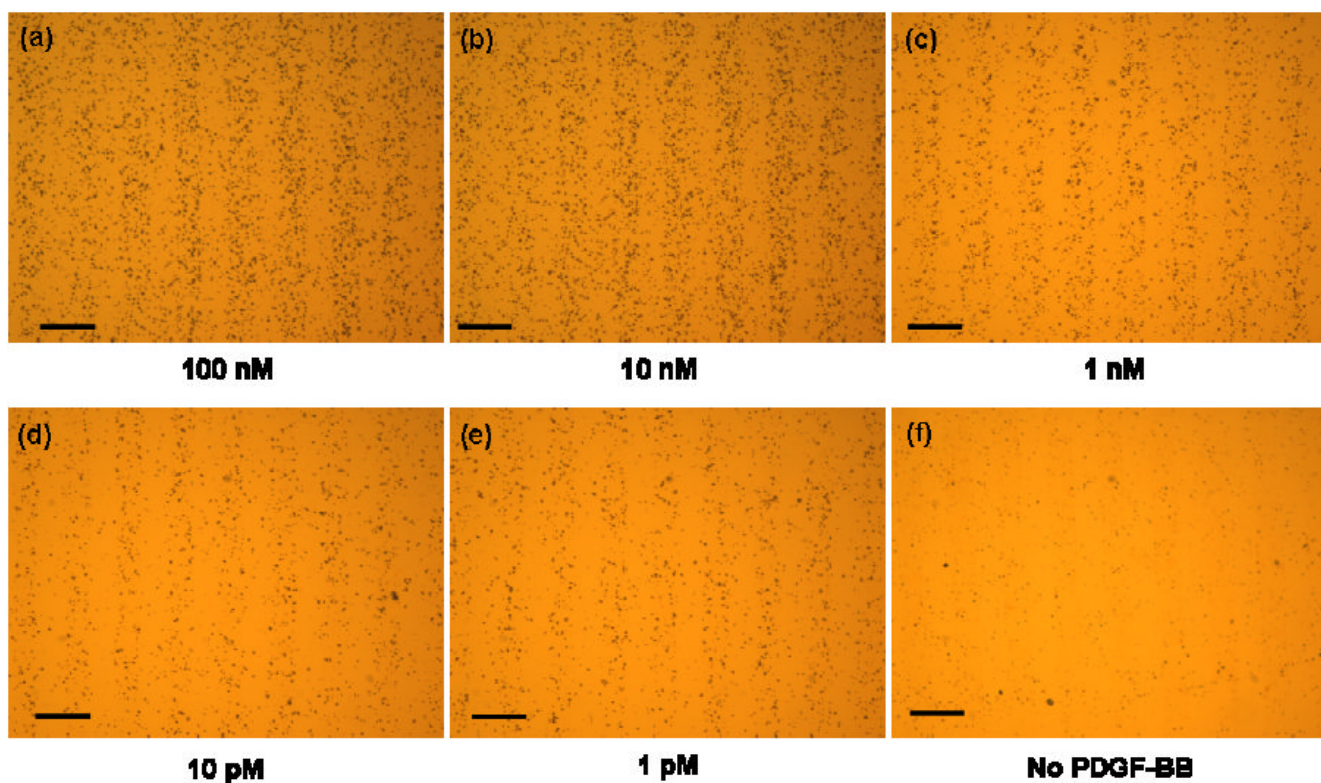


**Figure 2.**  
(a)-(e) Optical micrographs of the self-assembled diffraction gratings formed by streptavidin-labeled beads with varying PDGF-BB concentration (10 pM – 100 nM). (f) Grating with no PDGF-BB.

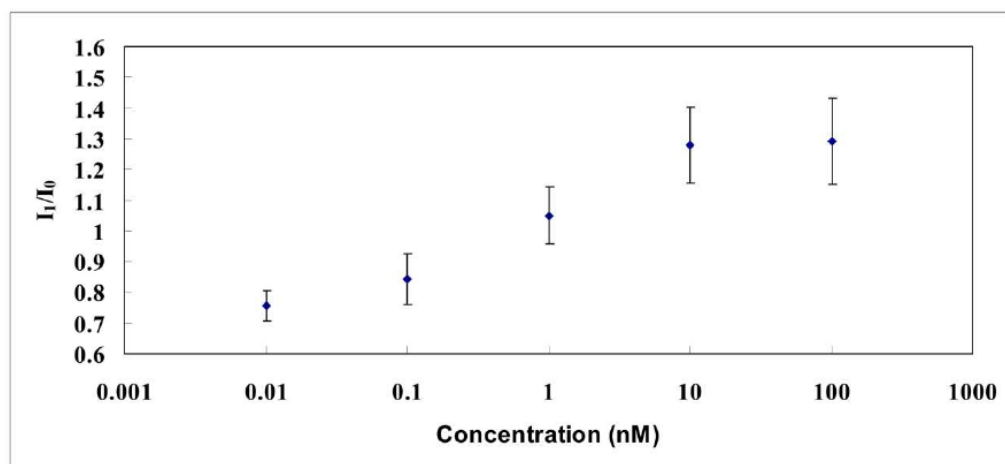


**Figure 3.** Variation of the normalized diffraction intensity ( $I_1/I_0$ ) with the PDGF-BB concentration (10 pM to 100 nM). Measurement was performed on 5 different areas, producing an average number of the normalized diffraction intensity ( $I_1/I_0$ ).

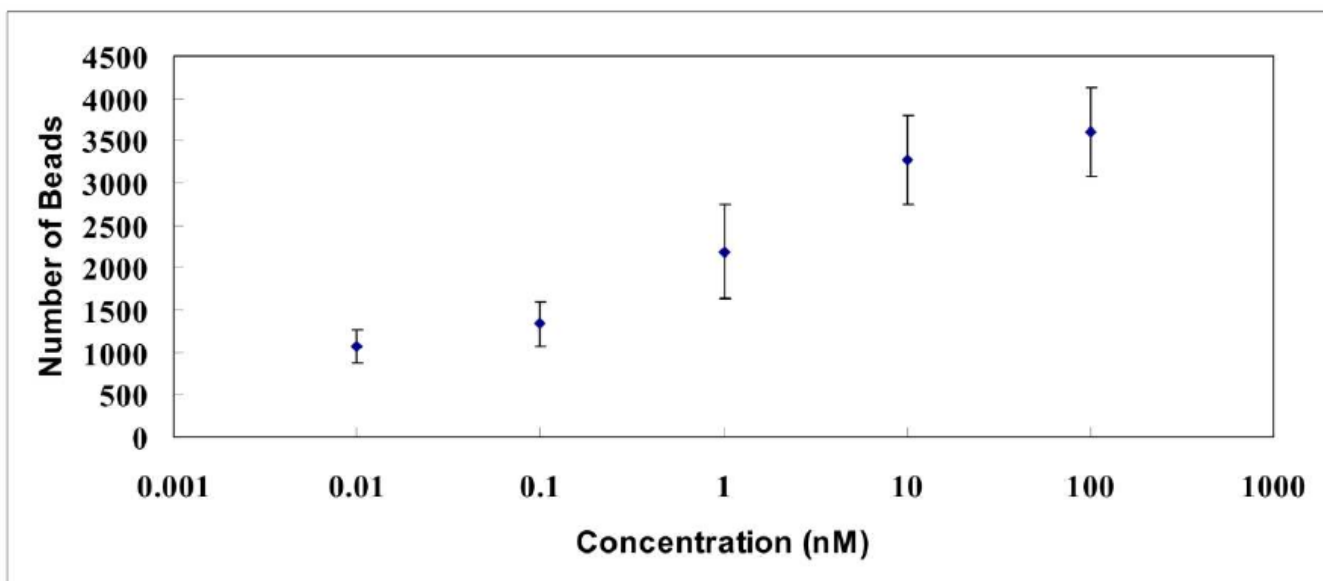


**Figure 4.** Variation of the number of beads with PDGF-BB concentration (10 pM – 100 nM). The counting was performed on five different areas on the chip, yielding an average number of beads.

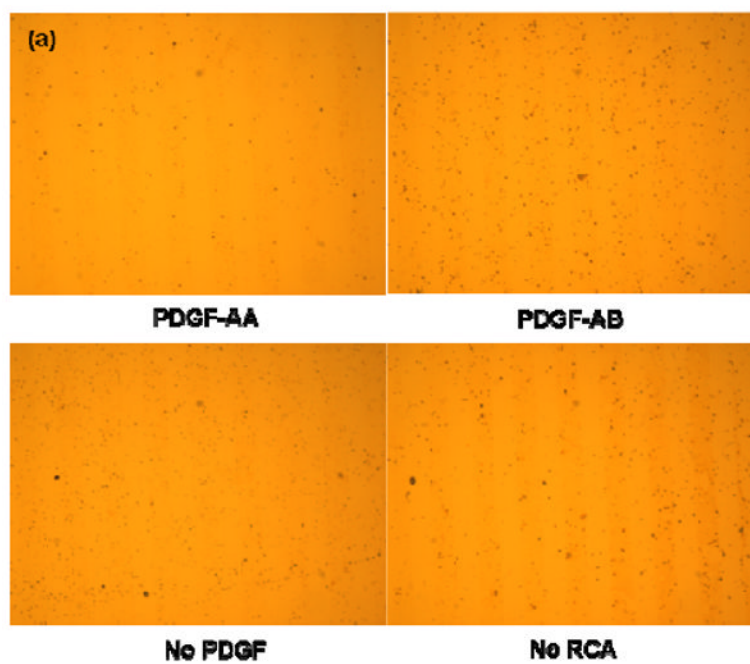


**Figure 5.**  
Optical micrographs of control chips to demonstrate the specificity of PDGF-BB detection.

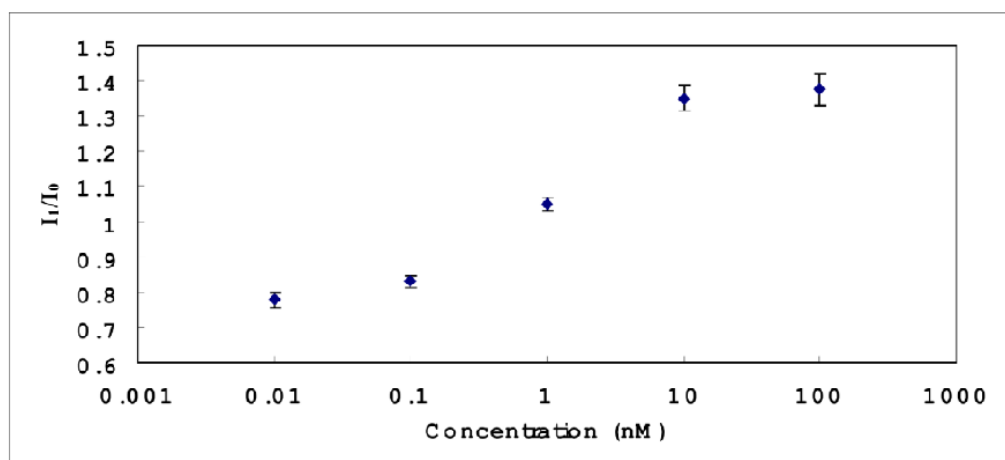


**Figure 6.** Variation of the normalized diffraction intensity ( $I_1/I_0$ ) with the PDGF-BB concentration (10 pM to 100 nM). Measurement was performed on the same area three times where diffraction gratings were well-defined and robust.



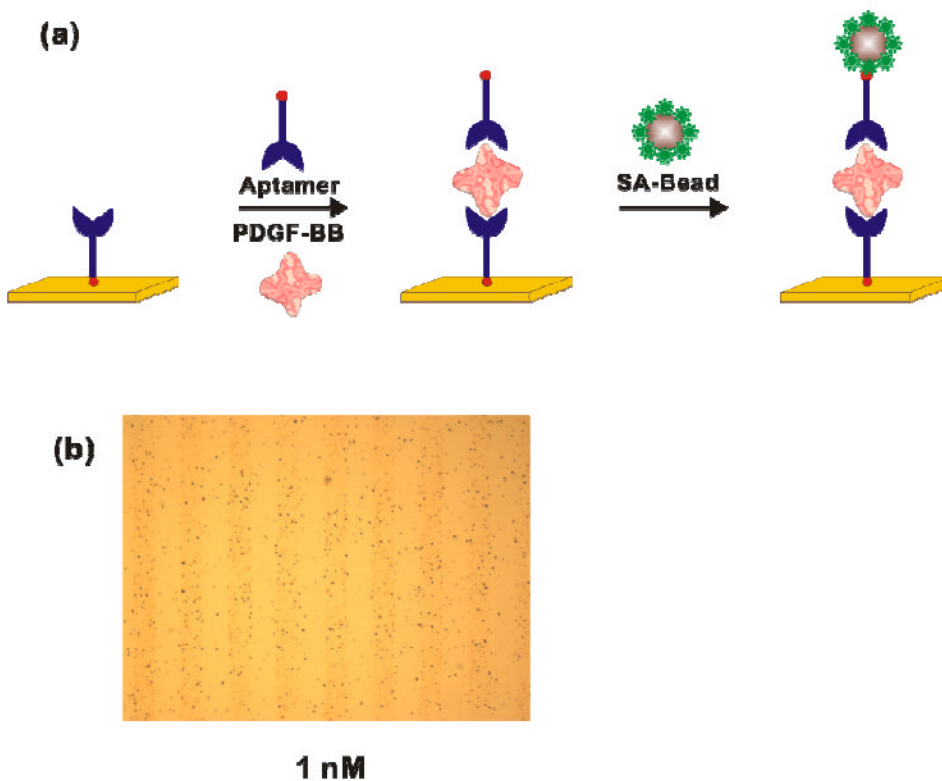


**Figure 7.** (a) Schematic of microbead-based aptamer sandwich assay without RCA. Biotinylated aptamer was immobilized on streptavidin functionalized periodic patterns. PDGF-BB was introduced, and sandwiched by another biotinylated aptamer. Streptavidin conjugated magnetic beads bound to free biotins of the aptamers that were captured by PDGF-BB. (b) Optical micrograph of the chip with 1 nM PDGF-BB.